Preparation and Characterization of Fluorescent Polymer Magnetic Particles

H. Baharvand

Polymer Science Department, Iran Polymer and Petrochemical Institute, Tehran, Iran

Received 17 November 2007; accepted 20 February 2008
DOI 10.1002/app.28328
Published online 28 April 2008 in Wiley InterScience (www.interscience.wiley.com).

ABSTRACT: Magnetic iron oxide (maghemite, Fe_3O_4) particles were encapsulated with fluorescent polymer phase. The resulting fluorescent magnetic polymer particles were characterized by Fourier transform infrared spectroscopy (FTIR), thermal gravimeter analysis (TGA), reflection optical microscopy, differential scanning calorimeter (DSC), Fritsch particle sizer, scanning electron microscopy (SEM), powder X-ray diffractometer (XRD), and vibrating sample magnetometer (VSM) measurements. FTIR and XRD confirmed the presence of iron oxide in polymer phase. The TGA and DSC measurements indicated that the magnetic polymer particles have more than 50% iron oxide content and high thermal stability. SEM and reflection optical microscopy under UV light revealed that all maghemite particles were embedded in the polymer spheres and have fluorescent characteristics. The size-distribution analysis of prepared magnetic particles was shown that the means diameter of the particles slightly increased. According to our magnetometry data, shape of the loops evidences the ferromagnetic character of the material and no evidence of superparamagnetism was seen. © 2008 Wiley Periodicals, Inc. J Appl Polym Sci 109: 1823–1828, 2008

Key words: fluorescent magnetic polymer particle; iron oxide; encapsulation; polyester; polymerization

INTRODUCTION

Inorganic-polymer composites have recently been receiving growing attention. Several kinds of small inorganic particles have been coated with a layer of polymer or encapsulated in a polymer matrix. If these inorganic particles possess functions such as magnetic susceptibility, electrical conductivity, catalytic activity, or electroactivity, it may be possible to form functional composites from them. A great deal of effort has been devoted to creating water-based magnetic dispersions.[1,2] Magnetic polymer particles are used in several applications, for instance, detoxification of biological fluids, magnetic guidance of particle systems for specific drug-delivery processes and magnetic nondestructive inspection test. These magnetic polymer particles can be prepared using various strategies.

An old and simple method is coating or encapsulation of magnetic particles with preformed polymers. The magnetic particles and polymer materials are synthesized separately and then mixed together. Adsorption (physical or chemical) of either the magnetic particles onto the polymer spheres[3–5] or polymer onto the magnetic core[6] results in a composite particle with magnetic properties. Another method to obtain magnetic polymer dispersions is based on *in situ* precipitation of magnetic material in the presence of polymer. Ugelstad et al.[7] obtained magnetic particles by *in situ* precipitation of magnetic oxides within pores of preformed monodisperse, porous polystyrene seed. To achieve the encapsulation of inorganic particles, more suitable methods have been developed, including conventional emulsion or microemulsion polymerization in the presence of magnetic nanoparticles.[8–10] In the emulsion polymerization process, the monomer is dispersed in an aqueous solution of a surfactant and polymerization is started by a water-soluble initiator. Polymer particles can be formed by either homogeneous or heterogeneous nucleation, depending on the degree of water solubility of the monomer and the amount of surfactant used. In the presence of inorganic particles dispersed in the aqueous phase, an additional site can be the surface of the particles. The complexity of the nucleation mechanism and the difficulty in controlling the dispersion stability of inorganic particles during emulsification and polymerization appear to be the major obstacles to using this method successfully.[11–14] Recently, a new type of polymerization process, termed miniemulsion polymerization, has been the focus of research as an alternative to conventional emulsion polymerization. Miniemulsion polymerization is the subject of numerous theoretical[15–18] and experimental studies.[19–24,29] In

Correspondence to: H. Baharvand (baharvand@zworg.com).

Contract grant sponsor: Iran National Science Foundation (IRAN); contract grant number: 83023.

TABLE I
Typical Recipe Used for the Encapsulation of Iron Oxide

Water	160 mL
NaOH	0.87 g
Polyester resin	17.74 g
Styrene	10.6 g
Fluorescent pigment	12 g
Iron oxide	42.28 g
Span 80	3.71 g
Tween 80	1.5 g
AIBN	0.9 g

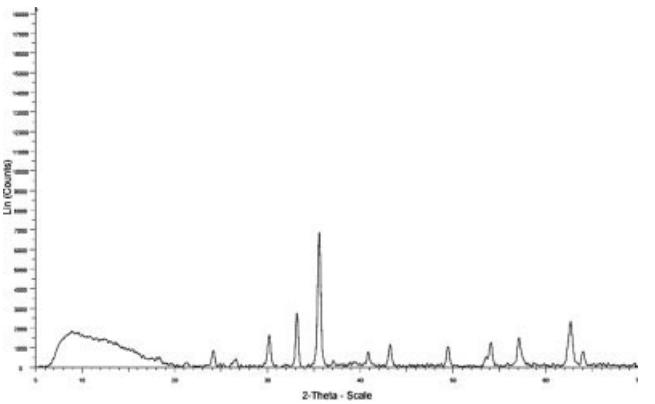

Figure 2 Powder XRD pattern for iron oxide.

miniemulsion polymerization, both the particle nucleation and the subsequent propagation reaction occur primarily in submicrometer monomer droplets. Each of these droplets can be regarded as an individual nanophase reactor.[25] Miniemulsion is typically obtained by shearing a system-containing monomer, water, surfactant, costabilizer, and initiator. The droplet diameter is adjusted by the type and amount of surfactant and costabilizer, the volume fraction of the disperse phase, and the homogenization process. Under very strict experimental conditions the miniemulsion can be polymerized without a change of particle identity. However, our knowledge of the fundamental processes involved in the preparation and polymerization of monomer miniemulsion is still limited. For example, the effect of homogenization conditions on the droplet size distribution and the mechanisms of droplet nucleation are still poorly known. Many new applications, however, have been discovered in the last few years. One of the characteristic features of the miniemulsion polymerization technique may be an advantageous encapsulation method. Potential advantages include the ability to control the size via formulation of the miniemulsion, directly dispersing the hydrophobic inorganic particles in the monomer phase, the ability to nucleate all the droplets containing inorganic particles, and faster polymerization.

The objective of this work was to obtain fluorescent iron oxide/polyester composite particles with a high magnetic content by miniemulsion polymerization technique. The composite particles were characterized by means of FTIR, TGA, DSC, Fritsch Particle Sizer, SEM, XRD, and VSM.

EXPERIMENTAL

Materials

The following chemicals were used: styrene (St; Merck); unsaturated polyester resin (BUSHEPOL 81715) was purchased from Emam Petrochemical Company (I.R. IRAN), azobisisobutironitrile (AIBN; Fluka), iron oxide (Bayer 686), sodium hydroxide (Merck), Tween 80 (Merck), fluorescent pigment Sterling 710 from Sterling Color (UK), and Span80 (Merck).

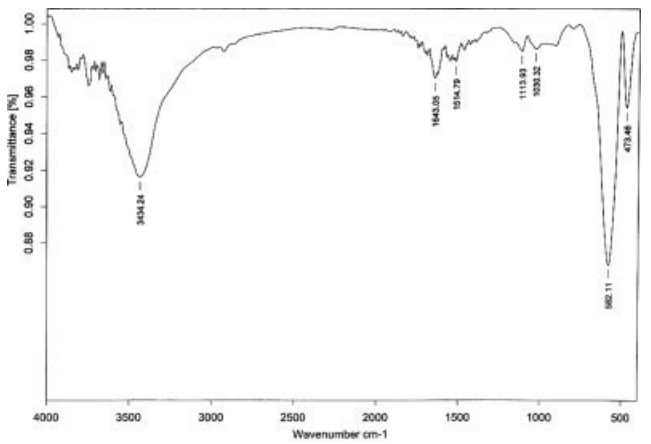

Figure 1 FTIR spectra of iron oxide.

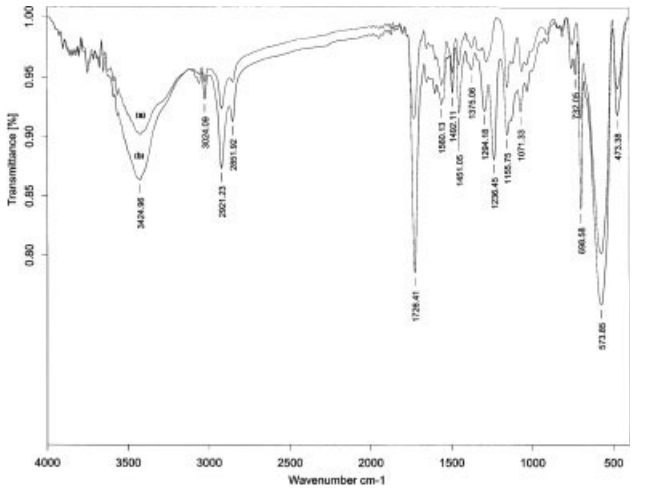

Figure 3 FTIR spectra of encapsulated iron oxide particles nonfluorescent (a) and fluorescent (b).

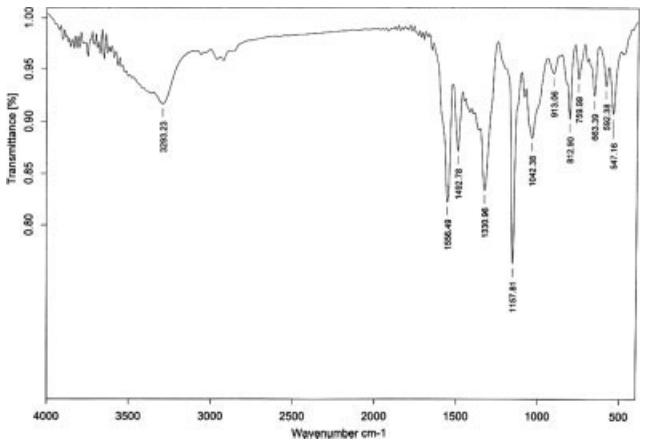

Figure 4 FTIR spectra of fluorescent pigment Sterling 710 from Sterling Color (UK).

Apparatus

The magnetic particle was examined using Fourier transform infrared spectroscopy (FTIR), Bruker, Equiker 55, morphology, and particle size measurements in the range of 0.5–100 μm were performed with reflection optical microscopy Jenaver (UK), scanning electron microscopy (SEM), Jeol JXA-840 and Fritsch Particle Sizer, ANALYSETTE 22. The iron oxide content of the polymer magnetic particle, the glass transition temperature, and degradation temperature of polymer phase were investigated by thermogravimetry analysis (TGA), PerkinElmer (pyrist 1) and differential scanning calorimetry (DSC), Netzsch DSC 200 F3; X-ray diffractmeter (XRD) with Siemens D500 instrument and vibrating sample magnetometer (VSM) with Princeton Applied Research VSM 155 instrument were taken to study structural and magnetic properties of the prepared particles respectively.

Procedure of encapsulation

A 250 cm^3 four-necked round-bottomed flask was equipped with a mechanical stirrer, thermometer, reflux condenser, and a nitrogen gas inlet and outlet. The flask initially charged with 160 mL deionized water and 0.87 g of sodium hydroxide. Then, at room temperature, the homogenized monomer phase containing unsaturated polyester resin, styrene, fluorescent pigment, iron oxide, span 80, tween 80, and AIBN (Table I) was added into the reaction flask, with continuous stirring. The stirring speed was fixed to 1000 rpm. After 30 min, the reaction flask was immersed into an 80°C oil bath, and the nitrogen gas was bubbled through the reaction mixture for deoxygenation. The polymerization was carried out at 80°C for 8 h. Then the reaction product was separated from the slurry by vacuum filtration. The filter cake was washed with deionized water for five times. Finally, the particles were dried at room temperature, and it was used to obtain the specimens for characterizations.

RESULTS AND DISCUSSION

Unlike conventional emulsion polymerization,[26] in which the principal site of particle nucleation is either in the aqueous phase or in the swollen monomer micelles in miniemulsion polymerization, the principal site of particle nucleation is monomer particle. So, using this technique, in the presence of inorganic particles, dispersed in the monomer phase, can only lead to encapsulated inorganic particles. In this work, similar to miniemulsion polymerization, the homogenized monomer phase-containing unsaturated polyester resin, styrene, AIBN, span 80, tween 80, and iron oxide particles was dispersed in water phase and polymerization was carried out.

FTIR and XRD methods were used to identify and characterization of iron oxide particles before and after encapsulation. FTIR spectra and powder XRD pattern of bare iron oxide were shown in Figures 1 and 2, respectively. Presence of double peak of 473 and 582 cm^{-1} in the FTIR spectra (Fig. 1) and presence of intensive sharp peaks at 33.15, 33.55, and 62.72° in the powder XRD pattern (Fig. 2) indicate maghemite structure of bare iron oxide particles.[27,28]

Reiteration characteristic peaks of maghemite in FTIR spectrum (Fig. 3) and XRD pattern (Fig. 5) of synthesized powder were shown the existence of an iron oxide in the synthesized particles and the fact that the structure of iron oxide after encapsulation was not changed.

Comparing FTIR spectrums for fluorescent and nonfluorescent particles (Fig. 3), it is not observed any differences, but the peaks in fluorescent sample

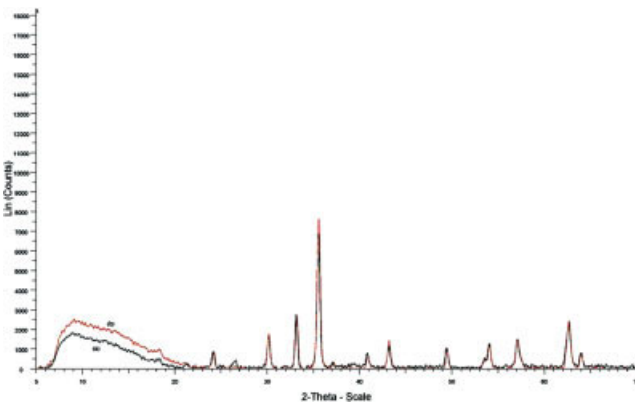

Figure 5 Powder XRD pattern for iron oxide (a) and encapsulated iron oxide (b). [Color figure can be viewed in the online issue, which is available at www.interscience.wiley.com.]

TABLE II
Surface Area Under Different Peak Regions in FTIR Spectrum

Peak region (cm^{-1})	Surface area
Nonfluorescent particles	
(Region 1) 1666–1530	1.34693
(Region 2) 1192–1089	1.20961
(Region 3) 1785–1667	3.70311
Fluorescent particles	
(Region 1) 1666–1530	1.13299
(Region 2) 1218–1096	0.934993
(Region 3) 1785–1667	1.63455

are more intensive. Knowing the fact that the peak of C=O group was not observed in FTIR spectrum of the fluorescent pigment (Fig. 4), the surface area of two peaks regions (region 1 and 2) in relation to the surface area of the peak region of three (Table II) for fluorescent and nonfluorescent samples were compared. It was seen that these two relations in fluorescent sample 1.9 and 1.7 times respectively, greater than that of nonfluorescent sample. This may be a reason for the presence of fluorescent pigment in the synthesized sample.

In the spectrum of Figure 3 were also observed:

- The peak with wave number of 1725 cm^{-1} in the FTIR spectra, which is the characteristic peak of polyester resins.
- The bands in the region 2800–3000 cm^{-1} corresponded to the CH_2 and CH_3 group of polymer backbone.
- The peak with wave number of 3025 and 3060 cm^{-1} corresponded to the C—H stretching of benzene ring.
- A broadband region of 3200–3600 cm^{-1} associated to the hydroxyl groups of iron oxide particles.

Morphology of the particles, before and after encapsulation of iron oxide, was studied by reflection optical microscopy and SEM. Optical micro-

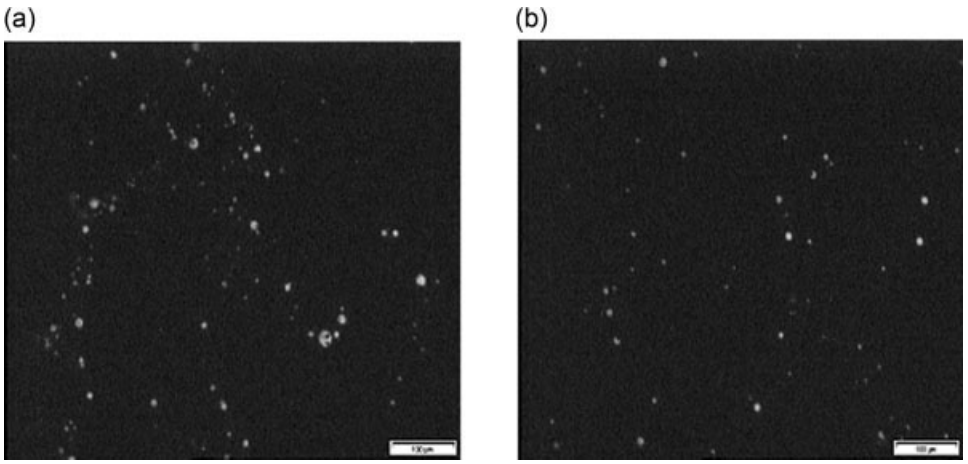

Figure 6 Optical micrograph of (a and b) fluorescent encapsulated iron oxide particles (100×).

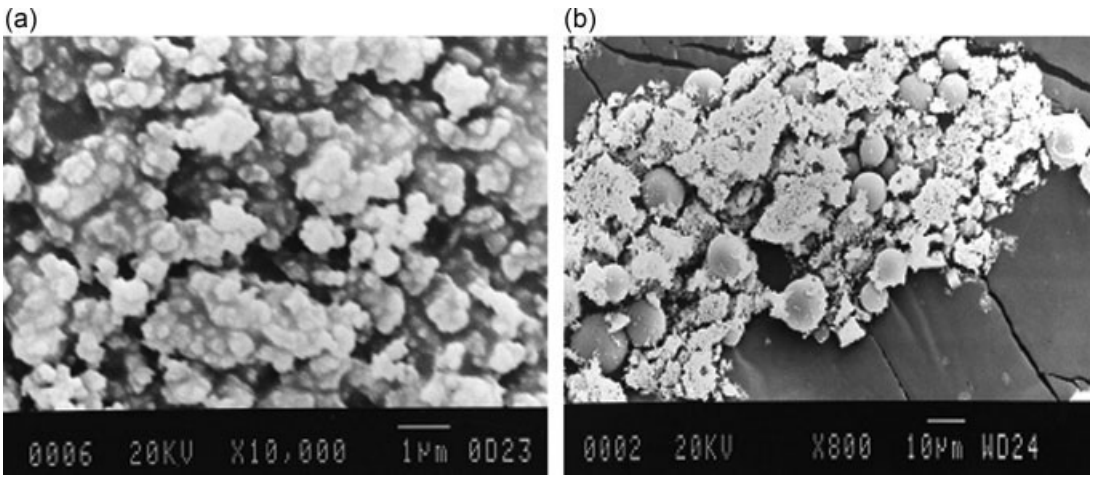

Figure 7 SEM micrograph of (a) iron oxide (10000×) and (b) encapsulated iron oxide (800×).

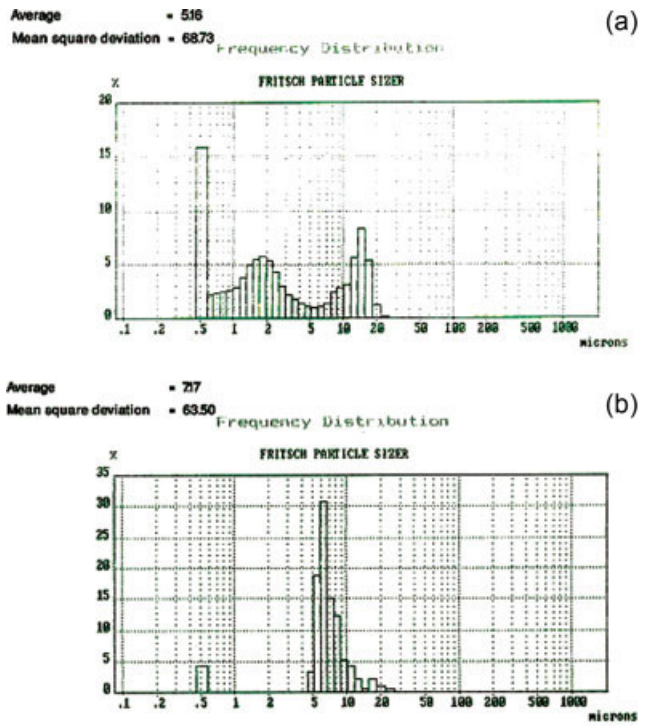

Figure 8 Particle size distribution of (a) iron oxide and (b) encapsulated iron oxide. [Color figure can be viewed in the online issue, which is available at www.interscience.wiley.com.]

graphs under UV light (wave length, $\lambda = 365$ nm) [Fig. 6(a,b)], and SEM micrographs [Fig. 7(a,b)] indicate that the iron oxide particles are shapeless and after encapsulation exhibited fluorescent characteristic and spherical forms.

Particle size measurements in the range of 0.5–100 μm were performed with Fritsch Particle Sizer. The size distribution analysis (Fig. 8) was shown that the mean diameter of iron oxide particles after encapsulation slightly increases. And it can be seen that the particle size distribution of iron oxide particle after encapsulation was shifted to larger size.

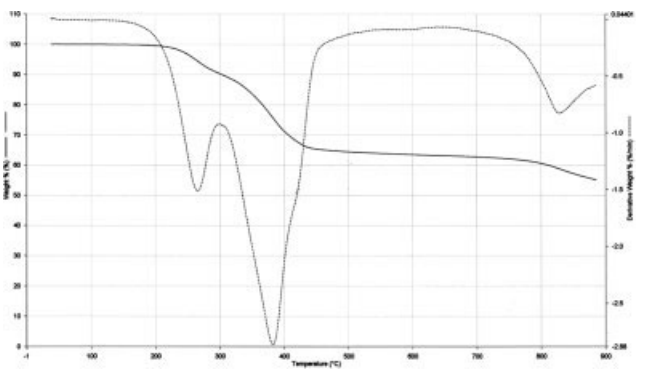

Figure 9 TGA thermogram of encapsulated iron oxide, in N_2, at heating rate of 10°C/min.

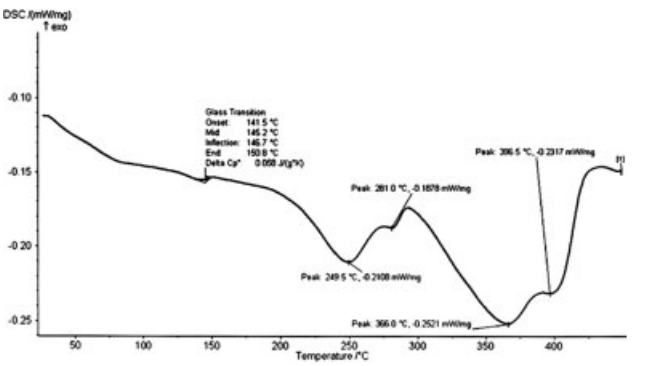

Figure 10 DSC thermogram of encapsulated iron oxide, in N2, at heating rate of 10°C/min.

Thermal behavior of the synthesized particles was studied by TGA and DSC. The TGA results can quantify iron oxide content and the thermal stability of polyester/iron oxide composite particles. Figure 9 shows the TGA results of synthesized particles. As it is seen, weight lose in TGA thermogram at between 200 and 300°C is related to the presence of adsorbed water, and dehyroxylation reaction ($2OH^- \rightarrow O^{2-} + H_2O$) of structural OH in the iron oxide and weight lose at between 300 and 500°C is due to the degradation of polymer phase. So the TGA measurements indicated the maximum concentration of the encapsulated iron oxide was 50% by weight and high thermal stability.

Figure 10 shows the DSC thermogram of polyester/iron oxide composite particles. It can be seen that the glass transition temperature (T_g) of polyester/iron oxide composite particles is about 145°C. As it is seen, there are two endothermic peaks in DSC thermogram at between 200 and 300°C and at between 300 and 500°C. First, endothermic peak is related to the release of adsorbed water, and dehyroxylation reaction of structural OH in the iron oxide and the second endothermic peak is due to the degradation of polymer phase. Absence of exothermic peak in DSC curve before degradation presents the absence of the residue monomer in the synthesized particles.

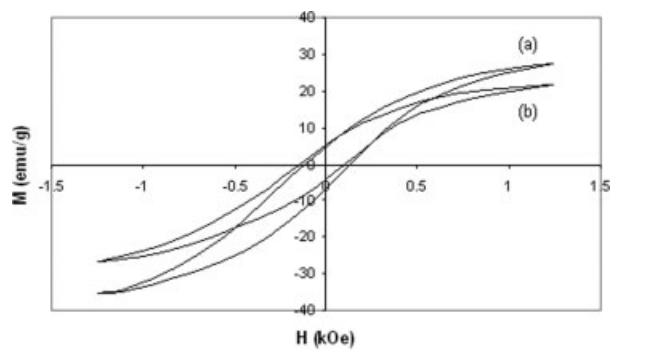

Figure 11 Hysteresis loops for the iron oxide (a) and composite particles (b).

The magnetic properties of the particles were determined by vibrating sample magnetometer (VSM). The hysteresis loops were recorded at room temperature are shown in Figure 11. The loops are closed and symmetrical versus origin of coordinate system. Shape of the loops evidences the ferromagnetic character of the material. No evidence of superparamagnetism was seen. Coercivity and remanence of the synthesized particles in comparison with the iron oxide particles slightly decrease. But their magnetic permeability considerably decreases. These variations may be due to the encapsulation of iron oxide particles with a polymer phase.

CONCLUSIONS

The maghemite core and fluorescent polyester shell composite particles were prepared by miniemulsion polymerization technique. Reflection optical microscopies under UV light, SEM, and particle size analysis of the resulting composite particles showed that these particles were fluorescent, regularly spherical core–shell morphology, and have narrower size distribution. The average particle diameter of composite particles was 7.17 μm. The TGA measurements indicated the synthesized particles have more than 50% iron oxide content and high thermal stability. DSC thermogram shows that the glass transition temperature (T_g) of polyester/iron oxide composite particles is about 145°C. The hysteresis loops were recorded at room temperature, using vibrating sample magnetometer (VSM), have shown the ferromagnetic character of the material.

References

1. Horak, D.; Semenyuk, N.; Lednicky, F. J Polym Sci Part A: Polym Chem 2003, 41, 1848.
2. Spanova, A.; Horak, D.; Soudkova, E.; Rittich, B. J Chromatogr B 2004, 800, 27.
3. Bizdoaca, E. L.; Spasova, M.; Farle, M.; Hilgendorff, M.; Caruso F. J Magn Magn Mater 2002, 240, 44.
4. Sauzedde, F.; Elaissari, A.; Pichot, C. Colloid Polym Sci 1999, 277, 1041.
5. Xulu, M.; Filipcsei, G.; Zrinyi, M. Macromolecules 2000, 33, 1716.
6. Jones, F.; Cölfen, H.; Antonietti, M. Colloid Polym Sci 2000, 278, 491.
7. Ugelstad, J; Mork, P. C.; Schmid, R.; Ellingsen, T.; Berge, A. Polym Int 1993, 30, 157.
8. Liu, Z. L.; Ding, Z. H.; Yao, K. L.; Tao, J.; Du, G. H.; Lu, Q. H.; Wang, X.; Gong, F. L.; Chen, X. J Magn Magn Mater 2003, 265, 98.
9. Xie, G.; Zhang, Q. Y.; Luo, Z. P.; Wu, M.; Li, T. H. J Appl Polym Sci 2003, 87, 1733.
10. Sauzedde, F.; Elaissari, A.; Pichot, C. Colloid Polym Sci 1999, 277, 846.
11. Marcianò, V.; Minore, A.; Turco Liveri, V. Colloid Polym Sci 2000, 278, 250.
12. Deng, Y.; Wang, L.; Yang, W.; Fu, S.; Elaıssari, A. J Magn Magn Mater 2003, 257, 69.
13. Banerjee, S.; John, V. T.; McPherson, G. L.; O'Conor, C. J.; Buisson, Y. S. L.; Akkara, J. A.; Kaplan, D. L. Colloid Polym Sci 1977, 275, 930.
14. Yang, Z. Z.; Qiu, D.; Li, J. Macromol Rapid Commun 2002, 23, 479.
15. Asua, J. M. Prog Polym Sci 2002, 27, 1283.
16. Asua, J. M. J Polym Sci Part A: Polym Chem 2004, 42, 1025.
17. Tronc, F.; Li, M.; Lu, J.; Winnik, A. M.; Kaul, L. B.; Graciet, J. C. J Polym Sci Part A: Polym Chem 2003, 41, 766.
18. Antonietti, M.; Landfester, K. Prog Polym Sci 2002, 27, 689.
19. Sood, A.; Awasthi, S. K. J Appl Polym Sci 2003, 88, 3058.
20. Landfester, K. Macromol Rapid Commun 2001, 22, 896.
21. Sajjadi, S.; Jahanzad, F. Eur Polym J 2003, 39, 785.
22. Limouzin, C.; Caviggia, A.; Ganachaud, F.; Hemery, P.; Macromolecules 2003 36, 667.
23. Luo, Y. W.; Schork, F. J. J Polym Sci Part A: Polym Chem 2002, 40, 3200.
24. Schork, F. J.; Poehlein, G. W.; Wang, S.; Reimers, J.; Rodrigues, J.; Samer, C. Colloids Surf A 1999, 153, 39.
25. Landfester, K.; Bechthold, N.; Foster, S.; Antinietti, M. Macromol Rapid Commun 1999, 20, 81.
26. Erdem, B.; Sudol, E. D.; Dimonie, V. L.; Mohamed, S. J Polym Sci Part A 2000, 38, 4441.
27. Poling, G.W. J Electro Chem Soc 1969, 116, 958.
28. Taylor, R. M.; Schwertmann, U. Clay Min 1974, 10, 299.
29. Schork, F. J.; Luo, Y.; Smulders, W.; Russum, J. P.; Butté, A. Adv Polym Sci 2005, 175, 129; DOI 10.1007/bl00115.